

Near-Optimal Method for Siting and Sizing of Distributed Storage in a Transmission Network

Hrvoje Pandžić, *Member, IEEE*, Yishen Wang, *Student Member, IEEE*, Ting Qiu, *Student Member, IEEE*, Yury Dvorkin, *Student Member, IEEE*, and Daniel S. Kirschen, *Fellow, IEEE*

Abstract—Energy storage can alleviate the problems that the uncertainty and variability associated with renewable energy sources such as wind and solar create in power systems. Besides applications such as frequency control, temporal arbitrage or the provision of reserve, where the location of storage is not particularly relevant, distributed storage could also be used to alleviate congestion in the transmission network. In such cases, the siting and sizing of this distributed storage is of crucial importance to its cost-effectiveness. This paper describes a three-stage planning procedure to identify the optimal locations and parameters of distributed storage units. In the first stage, the optimal storage locations and parameters are determined for each day of the year individually. In the second stage, a number of storage units is available at the locations that were identified as being optimal in the first stage, and their optimal energy and power ratings are determined. Finally, in the third stage, with both the locations and ratings fixed, the optimal operation of the storage units is simulated to quantify the benefits that they would provide by reducing congestion. The quality of the final solution is assessed by comparing it with the solution obtained at the first stage without constraints on storage sites or size. The approach is numerically tested on the IEEE RTS 96.

Index Terms—Energy storage, mixed-integer linear programming, storage siting, storage sizing, unit commitment.

I. INTRODUCTION

ENERGY storage can alleviate the problems that the uncertainty and variability associated with renewable energy sources such as wind and solar create in power systems [1]. However, as long as the cost of large capacity energy storage remains high, these devices will usually have to support multiple applications and hence provide multiple benefits to justify their deployment [2]. For some of these applications, e.g., frequency control, temporal arbitrage, or the provision of reserve, the location of the storage device does not significantly affect

the value that it provides. On the other hand, if storage is used to alleviate congestion or otherwise enhance transmission capacity, the siting and sizing of the devices determines their usefulness and hence their cost-effectiveness.

This paper proposes a framework for optimizing the location as well as the power and energy ratings of storage units distributed across a transmission network. Because they are distributed, these storage devices can perform a spatiotemporal arbitrage that alleviates network congestion and wind spillage, thus reducing the cost of producing energy using conventional generating units. Optimizing their location and size involves balancing the operational benefit that they provide against the cost of their deployment.

The optimal storage siting and sizing problem is similar to the transmission expansion problem. The only difference is that transmission lines move energy in space, while storage moves energy in time. For this reason, we use the same assumptions used in transmission expansion planning studies: new transmission assets are used to reduce congestion and enable large-scale integration of renewables.

A. Literature Review

The existing literature on energy storage in power systems can be divided into three categories: storage operation, storage sizing, and storage siting. Most of the papers published on this topic focus on storage operation. Given the energy and power ratings of a storage unit, the aim of these papers is to maximize the profit that independent power producers who own storage units can extract from the energy market. These models usually do not include transmission network constraints. Papers dealing with the problem of storage sizing are less common. They typically aim to find the optimal storage capacity at a predetermined location, usually next to a wind farm or a large load. Storage siting is the most complex of these three problems and has attracted the least amount of attention. The optimal storage size (i.e., energy and power ratings) depends on how this storage will be optimally operated. In turn, optimal storage siting depends on the size of the storage being considered and how it will be operated. This problem becomes even more complex if, instead of a single storage unit, distributed storage is considered. In this case, the number of storage locations is initially undefined.

1) *Storage Operation*: Varkani *et al.* [3] discuss the design of joint bidding by a wind farm and a pumped hydro plant in the day-ahead and ancillary services markets. The uncertainty of wind power generation is modeled using a neural network and the self-schedule is determined using stochastic programming. Garcia-Gonzalez *et al.* [4] propose another approach for joint

Manuscript received October 22, 2013; revised February 28, 2014, May 28, 2014, August 26, 2014, and October 17, 2014; accepted October 18, 2014. This work was supported in part by the ARPA-E Green Electricity Network Integration (GENI) program under project DE-FOA-0000473 and in part by the State of Washington STARS program. Paper no. TPWRS-01362-2013.

H. Pandžić is with the Faculty of Electrical Engineering and Computing University of Zagreb, Zagreb HR-10000, Croatia (e-mail: hrvoje.pandzic@ieec.org).

Y. Wang, T. Qiu, Y. Dvorkin, and D. S. Kirschen are with the Department of Electrical Engineering, University of Washington, Seattle, WA 98195-2500 USA (e-mail: ywang11@uw.edu; tqiu@uw.edu; dvorkin@uw.edu; kirschen@uw.edu).

Color versions of one or more of the figures in this paper are available online at <http://ieeexplore.ieee.org>.

Digital Object Identifier 10.1109/TPWRS.2014.2364257

market participation by a wind power plant and a pumped hydro storage plant. Their optimization model relies on a two-stage stochastic optimization where the day-ahead market prices and the wind generation are treated as random parameters. These authors show that the joint operation of a wind power plant and a pumped hydro plant achieves higher profits than the sum of the profits that they would obtain individually. The stochastic profit maximization of a virtual power plant, consisting of a pumped hydro storage unit, a photovoltaic power plant, and a conventional generating unit, is proposed in [5]. This model accounts for bilateral contracts and a day-ahead market. The conclusions emphasize the importance of an accurate assessment of the storage unit's energy and power ratings. A two-stage stochastic bidding model for a virtual power plant, consisting of a pumped hydro storage unit, a wind power plant, and a conventional generating unit, is proposed in [6]. In this model, a real-time market is used to balance the day-ahead market bids and the actual generation.

A method for scheduling and operating an energy storage unit supporting a wind power plant is proposed in [7]. A dynamic programming algorithm is used to determine the optimal electricity exchange, taking into account transmission constraints. However, only a single transmission line (the one that connects the bus to which the wind power plant and the energy storage are connected to the rest of the transmission network) is considered. The proposed method is suitable for any type of energy storage. Simulation results show that energy storage enables the owners of the wind power plant to take advantage of variations in the spot price, thus increasing the value of wind power in the electricity market.

Kim and Powell [8] derive an optimal commitment policy for wind farms coupled with a storage device. These authors consider conversion losses, mean-reverting energy prices, and a uniform distribution of wind energy.

Zhou *et al.* [9] investigate the problem of operating a wind farm, a storage unit and the transmission system. The system is modeled as a Markov decision process. They show that storage can substantially increase the monetary value of a system. For a typical scenario with tight transmission capacity, storage is reported to increase this value by 25%, of which 10% is due to reducing curtailment, 11% to time-shifting generation, and 4% to arbitrage. With looser transmission system constraints, storage is reported to increase the monetary value of the system by 21.5%, of which 0.5% is due to reducing curtailment, 17% to time-shifting, and 4% to arbitrage. In [10], the same authors investigate the operation of storage devices with different efficiencies in markets with frequent electricity surpluses, i.e., negative market prices.

Chandy *et al.* [11] formulate a simple optimal power flow model with storage, which captures some of the issues related to the integration of renewable sources and focuses on the effect that a single storage unit and a single generator have on the optimal power flow solution. The economic aspects of investment in storage are not considered.

Faghih *et al.* [12] discuss the optimal utilization of storage and the economic value of storage in the presence of ramp-rate constraints and stochastically varying electricity prices. They also characterize the price elasticity of the demand resulting

from the optimal utilization of storage. While the economic value of storage capacity is a non-decreasing function of price volatility, it is shown that due to the finite ramp rates, the value of storage saturates quickly as the capacity increases, regardless of price volatility. Finally, it is proven that optimal utilization of storage by consumers could induce a considerable amount of price elasticity, particularly around the average price.

An optimal operation strategy for a lossy energy storage system is presented in [13]. A multi-objective multi-period optimization is formulated using a model predictive control scheme, which relies on a linearized version of an adiabatic compressed air energy storage plant and respects *a priori* defined operational limits for the plant, i.e., power and energy constraints.

2) *Storage Sizing*: Harsha and Dahleh address the optimal storage investment problem in [14]. Their study focuses on a renewable generator aiming to support a portion of a local elastic demand by storing any excess generation. The goal is to minimize the long-term average expected cost of demand not served by renewable generation. The formulation treats the optimal storage investment problem as an average cost infinite horizon stochastic dynamic programming problem. The same authors study the optimal energy storage management and sizing problem in the presence of renewable energy and dynamic pricing [15]. The problem is formulated as a stochastic dynamic programming problem that aims to minimize the long-term average cost of conventional generation, as well as investment in storage, if any, while satisfying all the demand. These authors prove that under constant electricity prices storage is profitable if the ratio of the amortized cost of storage to the price of electricity is less than 1/4.

A probabilistic reliability assessment method for determining the adequate size of energy storage and transmission upgrades needed to connect wind generation to a power system is proposed in [16]. Energy storage is operated as a transmission asset. The paper focuses on the reliability impact of storage and its effect on the utilization of the available transmission capacity and does not address its economic value.

3) *Storage Siting*: Dvijotham *et al.* [17] have developed a heuristic algorithm for siting energy storage. Their approach places storage at all candidate buses and then solves a temporal optimization problem to determine the likely usage of the storage over a large range of renewable generation forecasts. Statistics describing usage patterns are used to reduce the number of storage devices.

Denholm and Shiohansi [18] examine the potential advantages of co-locating wind and energy storage to increase transmission utilization and decrease transmission costs. They demonstrate that co-locating a wind power plant and a storage unit decreases transmission requirements but also decreases the economic value of energy storage compared to when it is located at the load. They conclude that locating the storage at the wind farm is less attractive than locating it near the load if the storage device is able to take advantage of high-value ancillary or capacity services. Additionally, they conclude that the optimal size of co-located compressed air storage system is less than 25% of the rated wind power plant capacity.

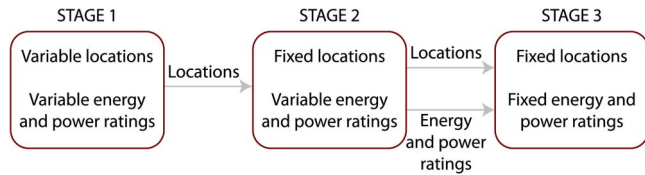


Fig. 1. Three-stage decomposition of the proposed storage siting and sizing problem.

B. Proposed Methodology and Contributions

In contrast with the papers discussed above, the methodology proposed in this paper captures both the economic and technical aspects of investment in storage. In addition, it considers not only the benefits for a specific wind farm, generating unit or load, but the system-wide effects.

In order to assess the benefits of investment in storage, at least an entire year of operation needs to be considered. However, solving a single unit commitment (UC) problem that determines optimal storage locations and parameters for a whole year is far beyond what is computationally doable at this point in time. Therefore, a UC problem is solved for each day of the year separately. We propose a three-stage decomposition of the problem, as shown in Fig. 1.

Stage 1: At the first stage, it is assumed that a storage device of unlimited energy and power ratings is available at each bus. Generator status from hour 24 is passed on to the following day as initial generator conditions, while the storage locations and ratings are independent from day to day. The objective function of this optimization problem takes into account both the operating cost of the system and the per diem cost of storage investment. In other words, a reduction in operating cost needs to justify the storage investment cost. The result of the first stage are optimal locations, as well as power and energy ratings, of storage installations for each day of the year. Obviously, this result has no real-world meaning because storage locations and ratings cannot be changed daily. However, comparing the UC costs achieved under these idealized conditions with the minimum cost achieved without storage devices gives the maximum possible operational savings that could be achieved by deploying storage. Furthermore, these results can be used as follows to identify storage locations that are most beneficial to the system. Buses are first ranked according to the number of days where the optimization decides to make use of some capacity at that location. A threshold number of days is then set and the buses where storage is used less often than this threshold are discarded from further consideration. The buses that are ranked above the threshold are deemed to be the most favorable locations for deploying storage and are passed on to Stage 2. Lowering this threshold increases the number of storage locations.

Stage 2: In the second stage, a UC problem is solved for each day of the year, once again taken individually, but this time storage is deemed available only at the locations identified at Stage 1. No constraints are placed on the energy and power ratings of these storage units during this optimization. Again, the generator data is passed on to the following day, while the storage ratings are independent from day to day. The maximum

energy stored and the maximum power injected or extracted determine the energy and power capacities for each storage unit for each day of the year. Daily storage and power capacities are averaged over the year to determine the energy and power ratings passed on to the Stage 3. While other metrics could be used to determine these ratings, experiments have shown that averaging gives the best results. Furthermore, using the average ratings facilitates the comparison between the results of Stages 2 and 3 because the overall investment costs remain the same.

Stage 3: At the third stage, the UC problem is again solved day-by-day for the whole year, but this time with fixed storage locations and ratings. At this stage, both the generator and the storage status is passed on to the following day. The results of this stage indicate the benefits that can realistically be achieved by deploying different amounts of storage. Comparing these results with those of the previous stages also provides an upper bound on the loss of optimality caused by the proposed decomposition.

The contributions of this paper can be summarized as follows:

- 1) The proposed approach determines the locations and ratings of distributed energy storage that maximize the system benefits of spatiotemporal arbitrage.
- 2) The method captures all the important aspects of the problem: seasonal variations in load and renewable energy generation, correlations between the productions of the wind farms or other stochastic renewable energy sources, conventional generator characteristics and locations, and transmission system constraints.
- 3) The benefits of investments in energy storage are unambiguously identified, which enables a rigorous assessment of different investment policies.

In this paper we assume that a benevolent, vertically integrated utility owns and operates all the distributed storage units, and can thus make all decisions regarding system planning and investments. If the electricity markets are sufficiently competitive, the results obtained from this perspective should provide a good indication of the location and amount of storage that merchant operators would deem profitable.

II. FORMULATION

The problem is formulated as a three-stage mixed-integer linear program and uses a lossless dc representation of the transmission network. Using a dc representation of power flows may result in up to 5% error in line loadings, but is justified in techno-economic and planning studies [19]. The error can be reduced by estimating losses *a priori* and including them in the load [20].

The following indices are used in the formulations of all three stages:

b	Index to the piecewise linear segments of the cost curve of a generating unit, from 1 to B .
i	Index to the set of generating units, from 1 to I .
j	Index to the set of start-up cost of generating units, from 1 to J .
l	Index to the set of transmission lines, from 1 to L .
s	Index to the set of buses, from 1 to S .
t	Index to the set of time periods in the optimization horizon, from 1 to T .

A. Stage 1

The objective function of Stage 1 for each day of the year is

$$\begin{aligned} & \text{Minimize} \\ & x_i(t), y_i(t), z_i(t), C_i(t), p_{i,b}(t), p_{i,b}^{\text{succ}}(t), w_{i,j}(t), \\ & SoC_s(t), ch_s(t), dis_s(t), SoC_s^{\text{max}}, ch_s^{\text{max}}, cw_w(t), \theta_s(t) \\ & \sum_{t=1}^T \sum_{i=1}^I C_i(t) + \sum_{s=1}^S (SoC_s^{\text{max}} \cdot IC_{en} + ch_s^{\text{max}} \cdot IC_{pow}). \quad (1) \end{aligned}$$

It minimizes the sum of the generation costs $C_i(t)$ of all the generators i over all time periods t and the daily investment cost in storage. The cost of investing in storage depends on both the energy and power ratings of the unit. The energy component is obtained by multiplying the maximum state of charge of each storage unit SoC_s^{max} (MWh) by the net present value of the daily investment cost per MWh, IC_{en} (\$/MWh). Similarly, the power component of this investment cost is the product of the maximum charge or discharge rate of the unit ch_s^{max} (MW) by the net present value of the daily investment cost per MW, IC_{pow} (\$/MW). These net present values are obtained by multiplying the energy and power rating costs by the daily capital recovery factors:

$$IC_{en} = c_{en} \frac{r \cdot (1+r)^h}{(1+r)^h - 1} \cdot \frac{1}{N_{year}} \quad (2)$$

$$IC_{pow} = c_{pow} \frac{r \cdot (1+r)^h}{(1+r)^h - 1} \cdot \frac{1}{N_{year}} \quad (3)$$

where c_{en} and c_{pow} are respectively the cost per MWh and per MW of a storage unit; h is the equipment lifetime; r is the annual interest rate; and N_{year} is the number of days in a year. The attractiveness of storage is dictated by the values IC_{en} and IC_{pow} , which depend on the cost per MWh and per MW of a storage unit, the storage lifetime and the annual interest rate.

The Stage 1 optimization is subject to the following constraints:

1) Constraints on the Binary Variables:

$$y_i(t_1) - z_i(t_1) = x_i(t_1) - g_i^{\text{on-off}} \quad \forall i \leq I \quad (4)$$

$$y_i(t) - z_i(t) = x_i(t) - x_i(t-1) \quad \forall 2 \leq t \leq T, i \leq I \quad (5)$$

$$y_i(t) + z_i(t) \leq 1 \quad \forall t \leq T, i \leq I. \quad (6)$$

Equations (4)–(6) relate the binary variables used to define the state of generator i : on-off status $x_i(t)$, start-up status $y_i(t)$ and shut-down status $z_i(t)$. These variables are equal to 1 if generator i is: 1) producing electricity; 2) started-up; 3) shut-down at time period t , and 0 otherwise, respectively. Initial generator on-off status is $g_i^{\text{on-off}}$.

2) Generator Output Constraints:

$$\begin{aligned} C_i(t) &= a_i \cdot x_i(t) + \sum_{b=1}^B k_{i,b} \cdot p_{i,b}(t) \\ &+ \text{suc}_i(t) \quad \forall t \leq T, i \leq I \quad (7) \end{aligned}$$

$$p_i(t) = \sum_{b=1}^B p_{i,b}(t) \quad \forall t \leq T, i \leq I \quad (8)$$

$$p_i(t) \geq g_i^{\text{min}} \cdot x_i(t) \quad \forall t \leq T, i \leq I \quad (9)$$

$$p_{i,b}(t) \leq g_{i,b}^{\text{max}} \cdot x_i(t) \quad \forall t \leq T, i \leq I, b \leq B. \quad (10)$$

Equation (7) defines the generation cost $C_i(t)$ as the sum of no-load generation cost, the variable generation cost and the start-up cost, $\text{suc}_i(t)$. The no-load cost, a_i (\$), is multiplied by the unit on-off status $x_i(t)$. The variable generation cost is calculated using piece-wise linear cost curves. The slope of segment b of generator i 's cost curve, $k_{i,b}$ (\$/MW), multiplies the power produced by that generator on this segment, $p_{i,b}(t)$ (MW). Constraint (8) defines the generator outputs, $p_i(t)$, as the sum of the power that it produces on each segment of its cost curve, $p_{i,b}(t)$. Constraints (9) and (10) impose minimum limits on generator outputs, g_i^{min} , and maximum limits, g_i^{max} , on each output segment $p_{i,b}(t)$.

3) Generator Minimum Up and Down Times:

$$x_i(t) = g_i^{\text{on-off}} \quad \forall t \leq L_i^{\text{up,min}} + L_i^{\text{down,min}}, i \leq I \quad (11)$$

$$\sum_{tt=t-g_i^{\text{up}}+1}^t y_i(tt) \leq x_i(t) \quad \forall t \geq L_i^{\text{up,min}}, i \leq I \quad (12)$$

$$\sum_{tt=t-g_i^{\text{down}}+1}^t z_i(tt) \leq 1 - x_i(t) \quad \forall t \geq L_i^{\text{down,min}}, i \leq I. \quad (13)$$

Constraint (11) sets on-off status for the first $L_i^{\text{up,min}}$ or $L_i^{\text{down,min}}$ (at least one of these is zero) time periods to be equal to the generator i on-off status, $g_i^{\text{on-off}}$, at $t=0$. $L_i^{\text{up,min}}$ is equal to $\max\{0, \min\{T, (g_i^{\text{up}} - g_i^{\text{up,init}}) \cdot g_i^{\text{on-off}}\}\}$ which is the number of time periods that generator i has to be on at the beginning of the optimization horizon. Analogously, $L_i^{\text{down,min}}$ is equal to $\max\{0, \min\{T, (g_i^{\text{down}} - g_i^{\text{down,init}}) \cdot (1 - g_i^{\text{on-off}})\}\}$. Parameter g_i^{up} is the minimum up time of generator i , while g_i^{down} is its minimum down time. $g_i^{\text{up,init}}$ is the time that generator i has been up before the first time period, and $g_i^{\text{down,init}}$ is the time that generator i has been down before the first time period. Constraints (12) and (13) enforce minimum up and down time for the remaining time periods.

4) Start-Up Costs:

$$\sum_{j=1}^J w_{i,j}(t) = y_i(t) \quad \forall t \leq T, i \leq I \quad (14)$$

$$\begin{aligned} w_{i,j}(t) &\leq \min\{t-1, \text{suc}_{i,j+1}^{\text{lim}}\} \\ &\sum_{tt=\text{suc}_{i,j}^{\text{lim}}} z_i(t-tt) \\ &+ 1\$ \left\{ j \leq J-1 \wedge \text{suc}_{i,j}^{\text{lim}} \leq g_i^{\text{down,init}} + t-1 < \text{suc}_{i,j+1}^{\text{lim}} \right\} \\ &+ 1\$ \left\{ j = J \wedge \text{suc}_{i,j}^{\text{lim}} \leq g_i^{\text{down,init}} + t-1 \right\} \\ &\forall t \leq T, i \leq I, j \leq J \quad (15) \end{aligned}$$

$$\text{suc}_i(t) = \sum_{j=1}^J w_{i,j}(t) \cdot \text{suc}_{i,j}^{\text{cost}} \quad \forall t \leq T, i \leq I. \quad (16)$$

Binary variable $w_{i,j}(t)$ is equal to 1 if generator i is started at time period t after being off for j time periods, and 0 otherwise. Equation (14) forces one j element of $w_{i,j}(t)$ to be equal to 1 if a generator is started at time period t , i.e., if $y_i(t) = 1$. Constraint (15) is used to determine which j element of $w_{i,j}(t)$ will be set to 1, depending on the number of time periods a generator

has been off. $\text{suc}_{i,j}^{\text{lim}}$ denotes the time limits of each segment of the stepwise j -segments start-up cost curve of generator i . The first term on the right-hand side determines the proper j element to be equal to 1 if a generator was last shut down within the optimization horizon. The second term is equal to 1 if a generator was last shut down up to J time periods before the current one, including the down time prior to the optimization horizon. The third term is equal to 1 if a generator has been shut down for J or more time periods, including the down time prior to the optimization horizon. Being shut down for J or more time periods results in the highest start-up cost. The actual start-up cost is determined in (16) by multiplying the binary variable $w_{i,j}(t)$ with the corresponding stepwise start-up cost values $\text{suc}_{i,j}^{\text{cost}}$.

5) Ramping Constraints:

$$-\text{ramp}_i^{\text{down}} \leq p_i(t_1) - p_i^0 \quad \forall i \leq I \quad (17)$$

$$\text{ramp}_i^{\text{up}} \geq p_i(t_1) - p_i^0 \quad \forall i \leq I \quad (18)$$

$$-\text{ramp}_i^{\text{down}} \leq p_i(t) - p_i(t-1) \quad \forall 2 \leq t \leq T, i \leq I \quad (19)$$

$$\text{ramp}_i^{\text{up}} \geq p_i(t) - p_i(t-1) \quad \forall 2 \leq t \leq T, i \leq I. \quad (20)$$

Constraints (17) and (18) enforce respectively the ramp down and ramp up constraints for the first time period, accounting for the generator output at $t=0$, p_i^0 . The ramping constraints for the remaining time periods are enforced by (19) and (20).

6) Storage Constraints:

$$\begin{aligned} \text{SoC}_s(t) &= \text{SoC}_s(t-1) + ch_s(t) \cdot \Delta t - dis_s(t) \\ &\quad \cdot \Delta t \quad \forall t \leq T, s \leq S \end{aligned} \quad (21)$$

$$\text{SoC}_s(t) \leq \text{SoC}_s^{\text{max}} \quad \forall t \leq T, s \leq S \quad (22)$$

$$ch_s(t) \leq ch_s^{\text{max}} \quad \forall t \leq T, s \leq S \quad (23)$$

$$dis_s(t) \leq ch_s^{\text{max}} \quad \forall t \leq T, s \leq S. \quad (24)$$

Equation (21) sets the storage state of charge, $\text{SoC}_s(t)$, at the end of time period t as a function of its state of charge at the end of the previous time period and of the charging or discharging that took place during time period t . Constraints (22)–(24) impose an upper limit $\text{SoC}_s^{\text{max}}$ (MWh) on the state of charge, and ch_s^{max} (MW) on the rates of charge and discharge. Note that at Stage 1, these limits are treated as variables. Charging and discharging power limits are assumed to be equal.

When a storage technology does not support an independent choice of energy and power ratings, the first term in the brackets of the objective function (1) is discarded, and the following constraint is added:

$$\text{SoC}_s^{\text{max}} = R \cdot ch_s^{\text{max}} \quad \forall s \leq S \quad (25)$$

where R is the constant energy/power ratio for the storage technology that has been chosen.

7) Transmission Constraints:

$$\begin{aligned} &\sum_{i=1|i \in S}^I p_i(t) + \sum_{w=1|w \in S}^W (aw_w(t) - cw_w(t)) \\ &- \sum_{\{s,m\} \in L|m > s} B_{sm} (\theta_s(t) - \theta_m(t)) \\ &+ \sum_{\{s,m\} \in L|m < s} B_{ms} (\theta_m(t) - \theta_s(t)) \end{aligned} \quad (26)$$

$$\begin{aligned} &+ dis_s(t) \cdot \eta_{\text{dis}} = d_s(t) + \frac{ch_s(t)}{\eta_{\text{ch}}} \quad \forall t \leq T, s \leq S \\ &- l_{sm}^{\text{max}} \leq B_{sm} (\theta_s(t) - \theta_m(t)) \leq l_{sm}^{\text{max}} \quad \forall t \leq T, \{s, m\} \in L \end{aligned} \quad (27)$$

$$-\pi \leq \theta_s(t) \leq \pi \quad \forall t \leq T, s \leq S \setminus s : \text{reference bus} \quad (28)$$

$$\theta_s(t) = 0 \quad \forall t \leq T, s : \text{reference bus.} \quad (29)$$

Equation (26) is the power balance constraint. $aw_w(t)$ is the available power output of wind farm w , while $cw_w(t)$ is a positive variable representing the curtailed wind output. B_{sm} is the admittance of the line connecting nodes s and m (S), and $\theta_s(t)$ is voltage angle at bus s (rad). $dis_s(t)$ and $ch_s(t)$ are the discharging and charging rates of storage at bus s , with charging and discharging efficiencies η_{dis} and η_{ch} . Demand at bus s is denoted with $d_s(t)$. Constraints (27) impose the limit l_{sm}^{max} on the line flows. Constraints (28) and (29) limit voltage angles and set the reference bus.

B. Stage 2

The Stage 2 model is identical to the Stage 1 model, with the exception of constraints (22)–(24), which are replaced by the following:

$$\text{SoC}_s(t) \leq \text{SoC}_s^{\text{max}} \cdot q_s \quad \forall t \leq T, s \leq S \quad (30)$$

$$ch_s(t) \leq ch_s^{\text{max}} \cdot q_s \quad \forall t \leq T, s \leq S \quad (31)$$

$$dis_s(t) \leq ch_s^{\text{max}} \cdot q_s \quad \forall t \leq T, s \leq S. \quad (32)$$

This formulation deploys storage only at selected buses by setting the binary parameter q_s to 1.

C. Stage 3

The Stage 3 model differs from the Stage 2 model only in treating $\text{SoC}_s^{\text{max}}$ and ch_s^{max} as fixed parameters, instead of variables.

III. CASE STUDY

A. System Data

The proposed approach was tested using the modified version of the IEEE RTS-96 [21] shown in Fig. 2 with an hourly time step. The generator data, including cost curves and conditions prior to the optimization horizon, are from [22]. We have added 19 wind farms with a total installed capacity of 6900 MW to this 73-bus, 96-generator, 51-load, and 120-line system. Table I lists the parameters of these wind farms: 3900 MW of wind power capacity are located in the western subsystem, 2400 MW in central subsystem, and only 600 MW in the eastern subsystem. The line ratings were reduced to 80% of their original values. This topography is intended to resemble ERCOT, where the West Zone contains most of the wind generation that needs to be evacuated to the metropolitan areas with high demand [23].

B. Wind Data

Wind power production was simulated for a whole year with a one-hour resolution using a time series model of wind speeds derived from NREL's Western Wind dataset [24]. This model provides 10-min wind speed and wind power data from 2004 to 2006 at 32 043 sites across the western USA. Each location is an

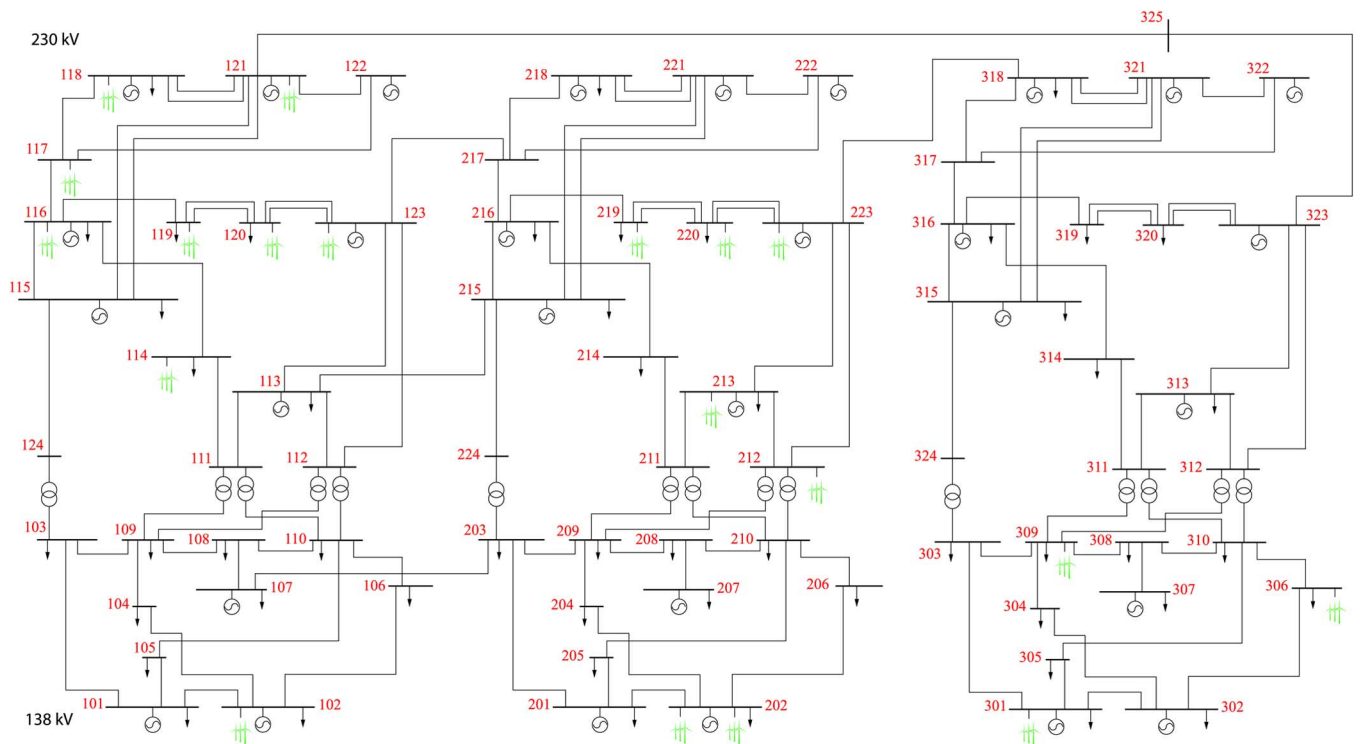


Fig. 2. Updated IEEE RTS-96.

TABLE I
WIND POWER PLANT DATA

Bus	Capacity (MW)	Annual utilization factor	Bus	Capacity (MW)	Annual utilization factor
101	300	35%	202	300	30%
114	300	33%	212	300	41%
116	600	35%	213	300	40%
117	600	33%	219	150	39%
118	300	26%	220	600	40%
119	600	37%	223	600	36%
120	600	38%	301	150	37%
121	300	27%	306	300	33%
123	300	36%	309	150	36%
202	150	33%			

artificial wind site with 10 aggregated Vestas V90-3MW wind turbines. Neighboring sites are grouped to build geographically correlated large capacity wind farms. Data from 2004 and 2005 is used to build the model, while data from 2006 is used for calibration.

The wind speed data is normalized by subtracting from each data point the average for the corresponding month and dividing it by the standard deviation for the corresponding hour of the month [25]. Then, the de-trended data is transformed into stationary Gaussian distributed series using empirical distribution function.

Next, the following time series models are fitted to this normalized data: AR(2), AR(3), ARMA(2,1), ARMA(3,1), and ARMA(3,2). Each model is adaptively updated every 6 hours based on the most recent 120 hours of wind data for 2006. After each update, each model provides a new 6-hour prediction.

This way, the resulting deterministic wind output captures the wind characteristics of all three years of available wind data.

Spatial correlation between the wind farms is implemented using a covariance matrix that generates spatially correlated random noise [26]. For each model, 100 estimates are generated based on this random noise, resulting in a total of 500 estimates every 6 hours. Applying an inverse transformation and adding the trend to each of these normalized estimates produces the actual wind speed dataset. The wind speed series is then converted into wind power series using a power curve derived from the original dataset. The final deterministic wind forecast is obtained averaging the 500 wind power estimates from the previous stage. The same procedure is used to obtain wind scenarios for the sensitivity analysis.

The final wind penetration varies by the hour and ranges from 0 to 126% of the hourly load. For comparison, in 2013 wind farms were generating more electricity than Denmark's needs during 258 hours, peaking at 142% on December 1, during the fifth hour [27]. Average available wind energy in the test system is 37% of the load. As a real-world comparison, in 2013 Denmark produced 28% of its electrical energy from wind farms, with a target of producing more than 50% of its electricity from wind farms by 2020 [28]. A similar increase is planned in Ireland, where the expected energy generated from wind by 2020 is 37% [29].

C. Storage Data

The following costs of storage devices are analyzed:

- 1) \$20/kWh and \$500/kW;
- 2) \$50/kWh and \$1000/kW;
- 3) \$100/kWh and \$1500/kW.

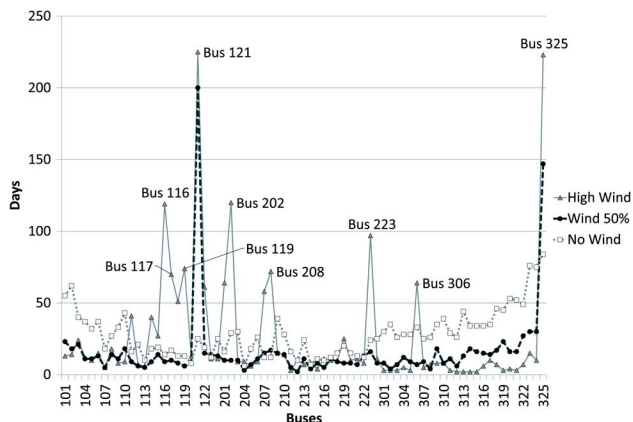


Fig. 3. Number of days in the year during which storage would be used at each bus according to the Stage 1 optimization (storage priced at \$20/kWh and \$500/kWh).

The expected battery lifetime is 20 years, and the interested rate is 5%. This data is used in (2) and (3) to calculate daily net present cost of storage investments.

Storage efficiency factors are 0.9 for both charging and discharging, resulting in a round-trip efficiency of 0.81.

D. Results for \$20/kWh and \$500/kWh

Based on these data, the Stage 1 optimal schedule results in a \$408 442 874 annual generation cost, which is a 2.46% reduction compared to the schedule that does not take advantage of storage devices. These devices also reduce the number of hourly committed generating units by 4.68%, i.e., from 148 487 to 141 533 annually. Wind curtailments decrease by 40%, from 1 342 283 MWh of spilled wind energy to 804 045 MWh.

Fig. 3 shows on how many days storage would be used at each bus. The most favorable storage locations include buses 121 (225 days), 325 (223 days), 202 (120 days), 116 (119 days), 223 (97 days), 119 (74 days), 208 (72 days), and 117 (70 days). Generally, these locations are near wind farms (e.g., buses 121, 202, 116) or along the corridors of high transit of wind generation towards large load centers (e.g., bus 325). On the other hand, at 60 out of 73 buses in the system storage would be used less than 50 days a year.

Fig. 3 also shows the results when available wind is reduced by 50% (18.6% penetration of wind energy) and without any wind. These curves are analyzed in Section IV-C.

Table II shows the locations that are considered in the Stage 2 storage optimization. The naming convention used to describe these locations is as follows. “sXXX” denotes the case where a single storage unit is located at bus XXX. “thrsYYY” denotes the case where storage is deployed at all the buses where storage is used more often than the threshold of YYY days per year. These thresholds have been chosen to bring about the inclusion of different number of storage locations.

Although the threshold rule is heuristic, it performs well because it considers the average benefit. For example, if a specific storage location is beneficial for a certain day and not for any other days, the benefit obtained on that single day is reduced or eliminated by mediocre performance on the other 364 days. On the other hand, if a specific location is favorable for

TABLE II
DESCRIPTION OF THE STAGE 2 CASES

Case	Buses with storage	Case	Buses with storage
s116	116	thrs100	116,121,202,325
s121	121	thrs80	116,121,202,223,325
s202	202	thrs74	116,119,121,202,223,325
s325	325	thrs72	116,119,121,202,208,223,325
thrs200	121,325	thrs70	116,117,119,121,202,208,223,325
thrs120	121,202,325		

storage placement during many days of the year, the overall benefit would be much higher than in the previous case. Additionally, the threshold rule is suitable for real-world applications because it enables a system planner to set the number of storage locations, which keeps the results in accordance to real plans and goals. The threshold selection analysis performed in this paper also provides valuable information on the minimum number of storage locations needed to achieve maximum savings.

Table III shows the results of Stage 1 and Stage 2. For each bus where storage is located, it gives the number of days during which storage would be used, the average of the maximum energy stored and the average of the maximum power injected or extracted. The results for Stage 1 assume that storage is available at all buses, not only at those listed. In all cases, the storage at bus 325 has the lowest capacity/power ratio, mostly below six. On the other hand, the storage at bus 116 has the highest ratio, usually above seven. Deploying storage at bus 121 would require the largest capacity, in terms of both energy and power. The reason for this is that the energy from this storage is used both to supply the load in the eastern subsystem via bus 325 and the load in the southern part of the western subsystem via bus 115. Bus 202 is suitable for storage placement because it accommodates two wind farms and is located next to the high-demand southern part of the central subsystem. Storage at this bus is used to mitigate wind volatility and to provide a steady power supply to the neighboring loads. As the threshold decreases, the number of storage units in the system increases, causing the total storage capacity to spread across the system, reducing the individual average storage capacities.

After running the Stage 2 model, the average of the daily maximum energy and power capacities are calculated and set as the storage ratings in the Stage 3 optimization. Using average daily capacities ensures that stages 2 and 3 assume the same investment costs and makes their results directly comparable. Fig. 4 shows the reduction in generation costs achieved at all three stages for different investment levels. Storage investment costs are calculated based on the energy and power ratings shown in Table III. Because they require the same investments, points on the Stage 2 and Stage 3 curves are vertically aligned. Investing \$50M into storage at bus 325 would reduce the generation expenses by 0.6%. Savings increase with the level of investment, but saturate as the number of storage locations increases. The Stage 3 curve, which represents solutions with fixed storage ratings, is just below the Stage 2 curve, indicating a minor loss of optimality. The savings achieved for cases thrs70, thrs72, thrs74, and thrs80 are almost identical to

TABLE III
RESULTS OF THE STAGE 1 AND STAGE 2 OPTIMIZATIONS
(STORAGE PRICED AT \$20/kWh AND \$500/kWh)

Case	Bus	Days	Avg. energy (MWh)	Avg. power (MW)	Ratio
Stage1	116	119	424	57	7.4
	117	70	55	8	6.9
	119	74	99	14	7.0
	121	225	541	77	7.0
	202	120	107	16	6.7
	208	72	18	3	6.1
	223	97	235	35	6.7
	325	223	225	37	6.1
thrs70	116	132	303	41	7.4
	117	90	117	17	6.9
	119	121	247	36	6.9
	121	258	629	93	6.8
	202	156	143	22	6.5
	208	129	76	12	6.2
	223	163	354	54	6.5
	325	273	243	41	5.9
thrs72	116	135	363	50	7.2
	119	127	238	35	6.7
	121	265	676	100	6.8
	202	155	148	22	6.6
	208	129	76	12	6.2
	223	163	358	55	6.5
thrs74	116	144	365	51	7.1
	119	124	246	36	6.8
	121	269	688	101	6.8
	202	178	167	26	6.5
	223	174	375	58	6.5
thrs80	116	170	504	71	7.1
	121	265	708	104	6.8
	202	173	219	34	6.5
	223	171	425	66	6.5
thrs100	116	167	597	85	7.0
	121	259	698	104	6.7
	202	195	318	49	6.6
	325	293	302	52	5.8
thrs120	121	285	1014	150	6.8
	202	201	403	60	6.8
	325	300	302	52	5.8
thrs200	121	295	1146	171	6.7
	325	304	354	60	5.9
s116	116	298	1393	204	6.8
s121	121	302	1128	168	6.7
s202	202	319	681	109	6.2
s325	325	328	457	84	5.4

the ideal savings achieved at Stage 1. This demonstrates that the heuristic decomposition involved in going from Stage 1 to Stage 2 and from Stage 2 to Stage 3 is valid.

Fig. 5 shows that investing in storage reduces the number of generating units online. However, this effect is not as linear as the one between the storage investment and the reduction in generation cost. Fig. 6 shows how investments in storage reduce the amount of wind curtailment. For this particular test case, the potential for reducing wind curtailment is 40% at Stage 2, and 20% at Stage 3, as compared to the base case without storage.

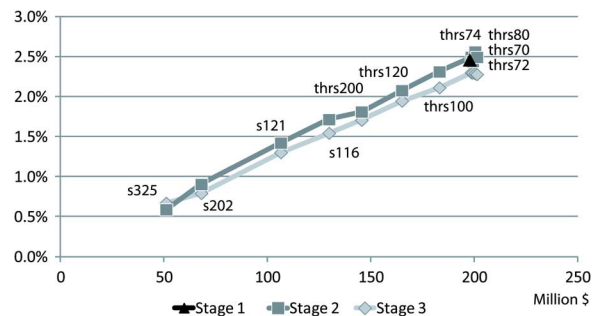


Fig. 4. Reduction in generation cost for different investment levels, as computed at the three optimization stages (storage priced at \$20/kWh and \$500/kWh).

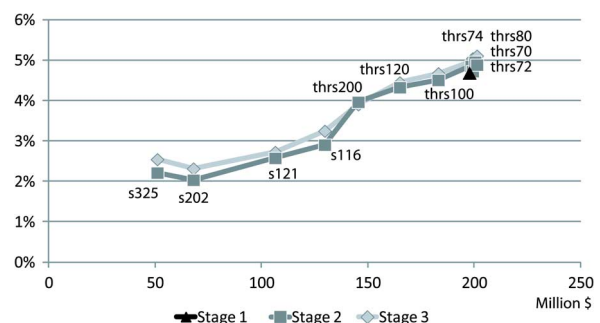


Fig. 5. Reduction in the number of generating units online for different investment levels, as computed at the three optimization stages (storage priced at \$20/kWh and \$500/kWh).

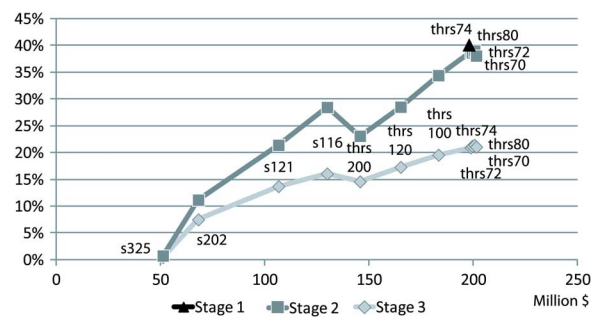


Fig. 6. Reduction in wind curtailment for different investment levels, as computed at the three optimization stages (storage priced at \$20/kWh and \$500/kWh).

To reduce the generation cost the optimization may sometimes find it more beneficial to reduce wind spillage and in other cases to reduce the number of units online.

Fig. 7 shows that the number of years required for investment in storage to break even ranges from 7.5 to 14.8 years, depending on the investment level. These breakeven periods assume that the only source of revenue for these storage installations is spatiotemporal arbitrage. In practice, the other benefits that distributed storage units can provide (such as ancillary services, deferral of transmission and generation investments, reduced generator cycling and maintenance costs) may reduce these breakeven periods.

Curves in Figs. 4–7 do not exhibit the classical saturation shape because they are the result of optimization procedures. They are truncated at around \$200M because the additional investments would not be justified by the additional savings in operating cost. Instead, the saturation manifests itself through

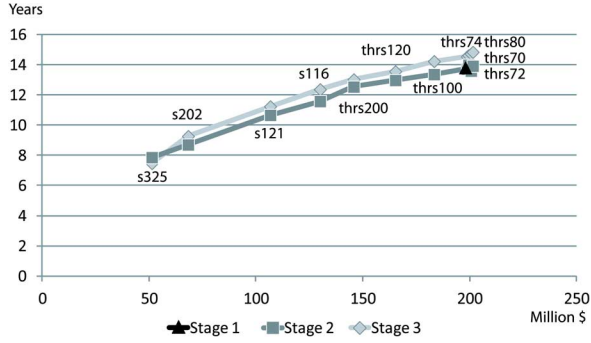


Fig. 7. Expected breakeven periods for different investment levels (storage priced at \$20/kWh and \$500/kWh).

TABLE IV
RESULTS OF THE STAGE 1 AND STAGE 2 OPTIMIZATIONS
(STORAGE PRICED AT \$50/kWh AND \$1000/kWh)

Case	Bus	Days	Avg. energy (MWh)	Avg. power (MW)	Ratio
Stage 1	121	65	4	1	4.1
	325	49	18	3	5.4
thrs49	121	146	50	10	5.0
	325	132	15	4	3.8
s121	121	157	48	10	4.9
s325	325	182	35	10	3.6

grouped results at the tails of the curves in Figs. 4–7. The minimum number of storage units that reach the point of saturation is five, as determined by the thrs80 case. This provides important information to a system planner: the maximum positive impact of distributed storage units is achieved with five storage units located at buses 116, 121, 202, 223, and 325.

E. Results for \$50/kWh and \$1000/kWh

Stage 1 results in \$418 053 227 annual generation cost, which is a 0.16% reduction as compared to the case with no storage devices. Modest savings, as compared to the previous case study, are the result of high storage investment cost. The sum of hourly committed units is decreased by 0.50%, and wind curtailment is reduced by 1.23%.

Number of days in which storages are used is significantly reduced as compared to the previous case study. The most favorable buses are 121 (65 days) and 325 (49 days). All the other buses use storage during less than 35 days throughout the year. For Stage 2 we consider three cases: s121, s325, and thrs49, implying storages at buses 121 and 325. Results of Stage 1 and Stage 2 models are presented in Table IV. Stage 1 results include other storage locations, apart from the ones listed in the table. Storage units have much lower energy and power ratings, as compared to the previous case study. The results show that in the s325 case, the storage is used during 182 days, which is exactly half of the year. In other cases, the storage utilization is even lower. This suggest that the benefit of storage at these prices is very low.

After running the Stage 2 model, average daily energy capacities and power ratings are calculated and fed to the Stage 3 model. Comparison of Stage 1, Stage 2, and Stage 3 reduction in generation cost, number of generating units online, and

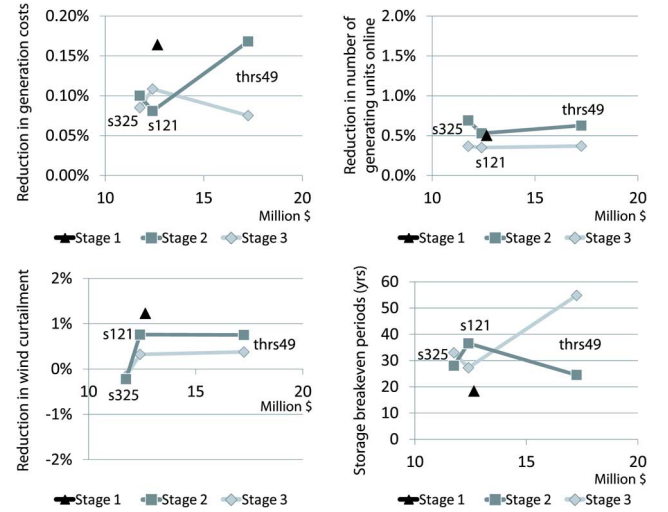


Fig. 8. Savings in generation costs (upper-left chart), reduction in the number of generating units online (upper-right chart), reduction in wind curtailment (lower-left chart), and expected breakeven periods (lower-right chart) for different investment levels, as computed at the three optimization stages (storage priced at \$50/kWh and \$1000/kWh).

wind curtailment for different investment policies is provided in Fig. 8. All the values are very low, besides the storage breakeven periods, which range from 19 years, for Stage 1, up to 55 years, for Stage 3 thrs49 case. These results indicate that the storage prices are too high to benefit from its utilization.

F. Results for \$100/kWh and \$1500/kWh

Storage investment costs are too high and no storage is used during any days throughout the year.

G. Computational Burden

All the simulations were carried out using CPLEX 12.1 running under the GAMS 23.7 [30] environment on an Intel i7 1.8-GHz processor with 4 GB of memory. The optimality gap was set at 0.6%. At each stage, a 36-hour UC is solved for each day of the year. The optimization for the following day is initialized based on the conditions at hour 24 of the previous day. This rolling horizon keeps the system in a favorable state for the following day.

The total computation time for Stage 1 was 22 hours, or 3 min 37 s per day. The overall Stage 2 computation time ranged from 9 hours for single storage cases up to 12 hours for the most demanding thrs70 case. Stage 3 required from 3.5 to 4 hours, depending on the case.

H. Sensitivity Analysis

A robust method for siting storage should be insensitive to small deviations in the expected wind output. To test whether this is actually the case, we performed a sensitivity analysis to quantify the effect of wind scenarios on the choice of storage locations. Fig. 9 compares the results of optimal storage locations presented in Fig. 3 with scenarios that result in approximately 5% lower, 1% lower, 1% higher, and 5% higher annual wind energy output. The results are almost identical and optimal

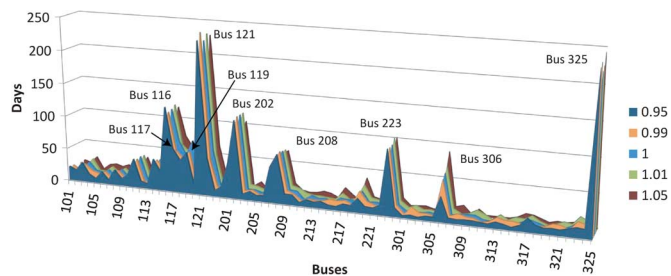


Fig. 9. Sensitivity analysis for different wind realizations of wind throughout the year (storage priced at \$20/kWh and \$500/kWh).

TABLE V

SENSITIVITY OF THE SAVINGS IN OPERATING COST TO CHANGES IN THE ENERGY AND POWER RATINGS FROM THE VALUES CALCULATED AT STAGE 2 (STORAGE PRICED AT \$20/kWh AND \$500/kWh)

Case	80% of the average	90% of the average	Average	110% of the average	120% of the average
s116	1.52%	1.54%	1.54%	1.43%	1.19%
s325	0.64%	0.66%	0.67%	0.58%	0.31%
thrs100	2.01%	2.08%	2.11%	1.82%	1.34%

locations match perfectly. This indicates that the proposed procedure is insensitive to small variations in wind realizations on annual basis.

At the end of Stage 2, we average the “optimal” energy and power ratings calculated for each day and use these quantities to set the ratings for the storage units. While this heuristic rule appears to work well, Table V shows the sensitivity of the net benefits to changes in the energy and power ratings of the storage units around the average annual values calculated based on the results of Stage 2. Using higher than average power and energy ratings rapidly decreases the benefits because of the higher investment costs. On the other hand, reducing the installed capacity decreases the savings in operating costs, but the reduced investment costs keep the overall benefits closer to the values achieved using the average power and energy storage ratings.

IV. ADDITIONAL ANALYSIS

In order to provide relevant conclusions on the performance of the proposed method, we provide an analysis of the impacts that congestion, the distribution of wind resources and the wind penetration level have on the results.

A. Impact of Congestion

In order to examine the impact of congestion, we ran a test case with no line flow limits, i.e., no congestion can ever occur. The results of Stage 1 are shown in Fig. 10. The results show that the most favorable storage locations are at buses 325 (208 days), 324 (165 days), and 323 (162 days). Based on this, we ran the following instances of Stage 2 optimization:

- 1) s325—storage allowed only at bus 325;
- 2) thrs165—storage allowed only at buses 325 and 324;
- 3) thrs160—storage allowed only at buses 325, 324, and 323.

Fig. 11 shows the differences between the daily operating cost of all three Stage 2 cases and the Stage 1 results. All the differ-

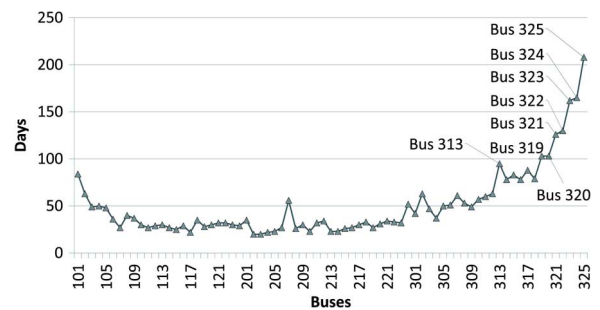


Fig. 10. Number of days in the year during which storage would be used at each bus according to the Stage 1 optimization for the case with no line flow limits (storage priced at \$20/kWh and \$500/kWh).

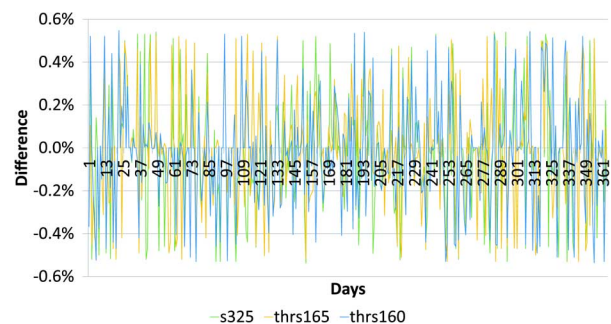


Fig. 11. Differences between daily operating cost of the three Stage 2 cases and Stage 1 results for the case of no line flow limits (storage priced at \$20/kWh and \$500/kWh).

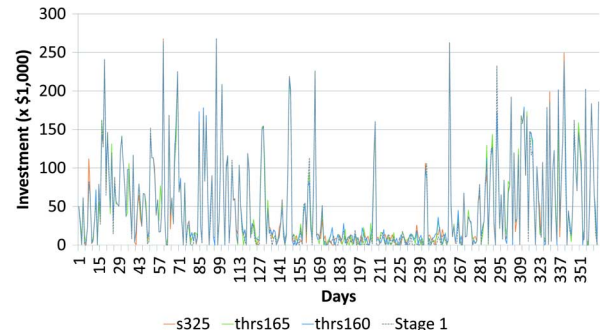


Fig. 12. Daily investment in storage for Stage 1 and three cases of Stage 2 for the case of no line flow limits (storage priced at \$20/kWh and \$500/kWh).

ences are within the 0.6% optimality gap used for all optimizations. This shows that the reduction in available storage locations from Stage 1 (all buses available) to Stage 2 (only one to three buses available, depending on the threshold) does not result in any loss of optimality.

Fig. 12 shows the daily investment in storage for Stage 1 and three cases of Stage 2. For most days the total investments are very close.

Table VI provides a detailed analysis of a randomly selected day (i.e., day 168). For this day, Stage 1 and s325 result in exactly the same installed storage energy and power capacity. However, in the Stage 1 solution storage is distributed across 15 buses, while in the s325 solution it is located at a single bus. Regardless of the location of storage, the Stage 1 and s325 solutions operate the storage in the same way and the overall cost is exactly the same.

TABLE VI
ANALYSIS OF DAY 168

	Stage 1	s325	thrs165	thrs160	Stage 1 (0% gap)
Objective function (\$)	1,097,392	1,097,392 (0%)	1,096,452 (-0.09%)	1,096,323 (-0.10%)	1,096,238 (-0.11%)
Storage energy capacity (MWh)	718.83	718.83	384.65	371.39	242.04
Storage power capacity (MW)	103.37	103.37	51.95	50.05	31.57
Daily investment in storage (\$)	14,563	14,563	7,421	7,155	4,547
Operating cost (\$)	1,082,829	1,082,829	1,089,030	1,089,169	1,091,691

On the other hand, thrs165 yields a solution with about half of the installed storage capacity. Although daily investment in storage is lower by over \$7000, the objective function value is less than a \$1000 lower because less storage results in a over \$6000 increase in operating cost. This indicates that different storage investment levels may result in very close values of the objective function (i.e., within the optimality gap). As a matter of fact, solving day 168 to zero optimality gap results in a value of the objective function of \$1 096 238, 242.04 MWh of storage energy capacity, and 31.57 MW of storage power capacity. However, this zero optimality gap optimization took over 3 hours for this single day. Observations similar to those for thrs165 case are also valid for the thrs160 case.

Based on this analysis, if the proposed procedure is applied to an uncongested network, it can only determine the optimal capacity of the storage, but not its location. From an operational perspective, this is arbitrary because the power extracted from any storage device can be used to supply any load in the network.

If the proposed method is applied to an uncongested network, the objective function is relatively flat around the optimum. This means that different investment levels can lead to very similar objective function values (e.g., 31.57 MW vs. 103.37 MW of storage in Table VI for Stage 1 with a 0% or 0.6% optimality gap). This issue can be identified based on very small changes between the base case (no storage) and Stage 1 solution. In the uncongested network test case presented in this subsection, this difference is only 0.62%. However, this problem can be eliminated by solving the model with a zero optimality gap, which would guarantee the global optimality of the solution.

As Fig. 13 demonstrates, even a slight amount of congestion makes the objective function much less flat.

B. Distribution of Wind Resources

To further examine the behavior of the proposed methodology, we ran a simulation with an even wind farm distribution across all three subsystems. Wind power plant capacities have been scaled to achieve an equal annual wind generation in all three subsystems. Stage 1 results are shown in Fig. 14. The most frequent storage locations are at buses 310 (268 days), 306 (185 days), 301 (136 days), and 202 (115 days). Based on the Stage 1 results, at Stage 2 we ran the following cases: s202, s301, s306, s310, thrs180 (buses 310 and 306), thrs130 (buses 310, 306, and 301), thrs100 (buses 310, 306, 301, and 202), thrs90 (buses 310,

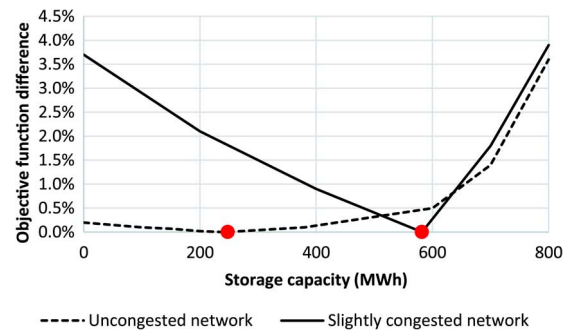


Fig. 13. Changes in objective function values around the global optimum for different installed storage capacities for uncongested and slightly congested network (day 168, storage priced at \$20/kWh and \$500/kWh).

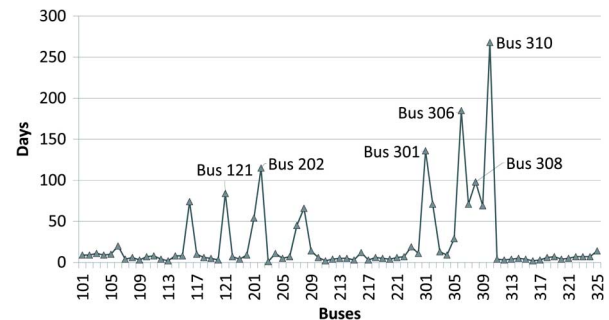


Fig. 14. Number of days in the year during which storage would be used at each bus according to the Stage 1 optimization for the case of even distribution of wind resources (storage priced at \$20/kWh and \$500/kWh).

306, 301, 202, and 308), and thrs80 (buses 310, 306, 301, 202, 308, and 121).

The reduction in generation costs achieved for the case with an even distribution of wind resources at all three stages for different investment levels are shown in Fig. 15. Stage 1 savings are 2.40%, which is slightly less than for an uneven wind resource distribution (2.46%). The total storage investments are lower when the distribution of wind resources is even: M\$187.5, as compared to M\$197.8 at Stage 1. Some of the favorable storage locations have changed as compared to the case of uneven distribution of wind resources. While buses 202 and 306 are still favorable for the installation of storage, buses 121 and 325 are no longer good choices because the even net load distribution reduces the loading of the line connecting buses 121 and 325, which was used to transfer wind power from the western to the eastern subsystem. These storage locations are now replaced by buses 301 and 310, where storage is used to buffer the transfer of wind power from the southern to the northern part of the eastern subsystem. These results indicate that the overall storage investment does not change significantly with the distribution of wind resources within the system, but the location and distribution of storage is dependent on the distribution of wind resources.

C. Level of Wind Penetration

Fig. 3 shows the most frequent Stage 1 storage locations for 50% and 0% wind penetration. As the wind penetration decreases, the storage locations are less distinctive and the overall savings are much lower. Stage 1 savings in the case of 50%

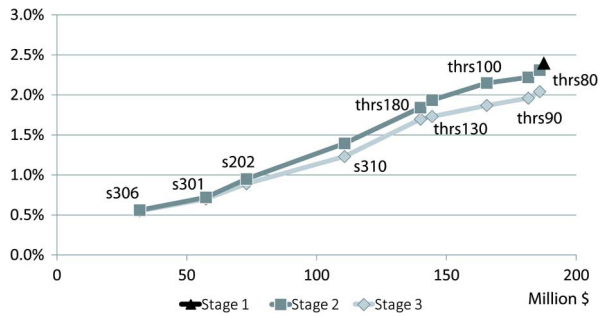


Fig. 15. Reduction in generation cost for different investment levels, as computed at the three optimization stages for the case of even distribution of wind resources (storage priced at \$20/kWh and \$500/kW).

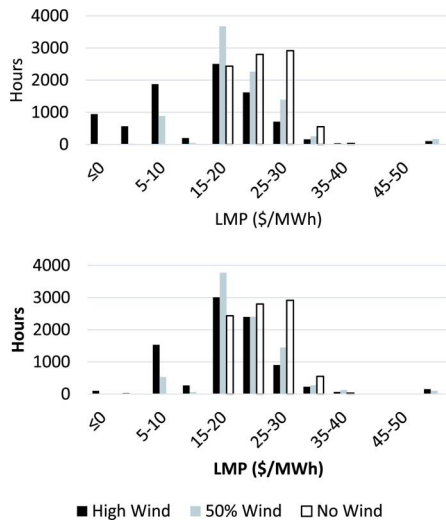


Fig. 16. Distribution of LMPs at bus 122 (upper graph) and bus 325 (lower graph) throughout the year for different wind penetration levels.

wind penetration are only 0.3%, while in the case of no wind generation they are only 0.1%. This indicates that the storage does not bring sufficient savings in operating costs to justify investments. This can be explained using the difference in locational marginal prices (LMPs). Fig. 16 shows the distribution of LMPs throughout the year for buses 122 (the one with the lowest average LMPs) and 325 (the one with the highest average LMPs). In the high wind case these LMPs take a wide range of values, from below 0 to over \$50/MWh. Furthermore, some of the LMPs are higher than the most expensive generation cost, e.g., over \$150/MWh. This phenomenon is explained in [31]. This range is smaller for the 50% wind case, while for the 0% wind case all the LMPs are between 15 and \$35/MWh. This shows that the volatility of LMPs over time is crucial for the economic attractiveness of storage installations.

V. CONCLUSIONS

The proposed technique for optimizing the siting and sizing of distributed storage units considers both the economic and technical aspects of the problem. A three-stage decomposition of the problem has been described. Stage 1 models an idealized problem where storage is available in any capacity at any node. Running this optimization day by day over a whole year helps

identify the locations where the spatiotemporal arbitrage that distributed storage units could perform would be most effective. Once these locations have been identified, they are passed on to the Stage 2 optimization, which takes them as given but leaves the energy and power capacities of the storage units unlimited. Averaging over a year the daily maxima of stored energy and injected or extracted power provides good values for the energy and power ratings of the storage units to be installed at these locations. Stage 3 models the fully constrained operation of the system including the storage units. Comparing the results of Stage 3 with those of the idealized situation considered at Stage 1 demonstrates that the heuristics resulting from the proposed decomposition do not cause a significant loss of optimality.

Based on extensive testing and analysis, the following conclusions are drawn:

- 1) The proposed method provides valuable information on the storage potential in a power system.
- 2) The computational burden of the method is reasonable as the storage siting and sizing analysis is performed independently of the current system operation.
- 3) When the network is not congested, the proposed procedure can be used to determine the optimal storage capacity, but the location of storage in such case would be determined by other factors.
- 4) The issue of the objective function flatness around the global optimum can be alleviated by solving the problem to zero optimality gap. Otherwise, it can be recognized by a very small change in objective function between the base case (no storage) and Stage 1 solution. In this case, a sensitivity check, such as in Fig. 13, needs to be done to assess the quality of the solution.
- 5) The overall storage investment does not change significantly with the distribution of wind resources within a system, but the location and distribution of storage is dependent on the distribution of wind resources.
- 6) The benefits of storage investments are directly correlated with the volatility of LMPs in a system.

REFERENCES

- [1] P. D. Brown, J. A. Pecos Lopes, and M. A. Matos, "Optimization of pumped storage capacity in an isolated power system with large renewable penetration," *IEEE Trans. Power Syst.*, vol. 23, no. 2, pp. 523–531, May 2008.
- [2] A. A. Akhil, G. Huff, A. B. Currier, B. C. Kaun, and D. M. Rastler, DOE/EPRI 2013 Electricity Storage Handbook in Collaboration With NRECA, Sandia National Lab., Rep. SAND2013-5131, Jul. 2013.
- [3] A. K. Varkani, A. Daraeipour, and H. Monsef, "A new self-scheduling strategy for integrated operation of wind and pumped-storage power plants in power markets," *Appl. Energy*, vol. 88, no. 12, pp. 5002–5012, Dec. 2011.
- [4] J. Garcia-Gonzalez, R. M. R. de la Muela, L. M. Santos, and A. M. Gonzalez, "Stochastic joint optimization of wind generation and pumped-storage units in an electricity market," *IEEE Trans. Power Syst.*, vol. 23, no. 2, pp. 460–468, May 2008.
- [5] H. Pandžić, I. Kuzle, and T. Capuder, "Virtual power plant mid-term dispatch optimization," *Appl. Energy*, vol. 101, no. 1, pp. 134–141, Jan. 2013.
- [6] H. Pandžić, J. M. Morales, A. J. Conejo, and I. Kuzle, "Offering model for a virtual power plant based on stochastic programming," *Appl. Energy*, vol. 105, no. 5, pp. 282–292, May 2013.
- [7] M. Korpaas, A. T. Holen, and R. Hildrum, "Operation and sizing of energy storage for wind power plants in a market system," *Elect. Power Energy Syst.*, vol. 25, no. 8, pp. 599–606, Oct. 2003.

- [8] J. H. Kim and W. B. Powell, "Optimal energy commitments with storage and intermittent supply," *Oper. Res.*, vol. 59, no. 6, pp. 1347–1360, Dec. 2011.
- [9] Y. Zhou, A. Scheller-Wolf, N. Secomandi, and S. Smith, Managing Wind-based Electricity Generation in the Presence of Storage and Transmission Capacity, Tepper School of Business, Paper 1477, 2013 [Online]. Available: repository.cmu.edu/cgi/viewcontent.cgi?article=2469&context=tepper
- [10] Y. Zhou, A. Scheller-Wolf, N. Secomandi, and S. Smith, Is It More Valuable to Store or Destroy Electricity Surpluses? Tepper School of Business, Paper 2012-E1 [Online]. Available: repository.cmu.edu/cgi/viewcontent.cgi?article=2470&context=tepper
- [11] K. M. Chandy, S. H. Low, U. Topcu, and H. Xu, "A simple optimal power flow model with energy storage," in *Proc. 49th IEEE Conf. Decision and Control*, Atlanta, GA, USA, Dec. 2010.
- [12] A. Faghih, M. Roozbehani, and M. Dahleh, "Optimal utilization of storage and the induced price elasticity of demand in the presence of ramp constraints," in *Proc. 50th IEEE Conf. Decision and Control and Eur. Control Conf.*, Orlando, FL, USA, Dec. 2011.
- [13] F. De Samanigo Steta, A. Ulbig, S. Koch, and G. Andersson, "A model-based optimal operation strategy for lossy energy storage systems: The case of compressed air energy storage plants," in *Proc. Power System Computation Conf.*, Stockholm, Sweden, Aug. 2011.
- [14] P. Harsha and M. Dahleh, "Optimal sizing of energy storage for efficient integration of renewable energy," in *Proc. 50th IEEE Conf. Decision and Control and Eur. Control Conf.*, Orlando, FL, USA, Dec. 2011.
- [15] P. Harsha and M. Dahleh, Optimal Management and Sizing of Energy Storage Under Dynamic Pricing for the Efficient Integration of Renewable Energy, working paper, 2012 [Online]. Available: web.mit.edu/pavithra/www/papers/Storage_HarshaDahleh2012.pdf
- [16] Y. Zhang, S. Zhu, and A. A. Chowdhury, "Reliability modeling and control schemes of composite energy storage and wind generation systems with adequate transmission upgrades," *IEEE Trans. Sustain. Energy*, vol. 2, no. 4, pp. 520–526, Oct. 2011.
- [17] K. Dvijotham, S. Backhaus, and M. Chertkov, Operations-Based Planning for Placement and Sizing of Energy Storage in a Grid With a High Penetration of Renewable, arXiv:1107.1382v2, Jul. 2011.
- [18] P. Denholm and R. Shiohansi, "The value of compressed air energy storage with wind in transmission-constrained electric power systems," *Energy Policy*, vol. 37, no. 8, pp. 3149–3158, Aug. 2009.
- [19] K. Purchala, L. Meeus, D. Van Dommelen, and R. Belmans, "Usefulness of DC power flow for active power flow analysis," in *Proc. IEEE PES General Meeting*, San Francisco, CA, USA, June 2005.
- [20] T. N. Santos and A. L. Diniz, "A dynamic piecewise linear model for DC transmission losses in optimal scheduling problems," *IEEE Trans. Power Syst.*, vol. 26, no. 2, pp. 508–519, May 2011.
- [21] The IEEE Reliability Test System—1996, "A report prepared by the Reliability Task Force of the Application of Probability Methods Subcommittee," *IEEE Trans. Power Syst.*, vol. 14, no. 3, pp. 1010–1020, Aug. 1999.
- [22] H. Pandžić, T. Qiu, and D. Kirschen, "Comparison of state-of-the-art transmission constrained unit commitment formulations," in *Proc. IEEE PES General Meeting*, Vancouver, BC, Canada, July 2013.
- [23] R. Baldick, "Wind and energy markets: A case study of Texas," *IEEE Syst. J.*, vol. 6, no. 1, pp. 27–34, Mar. 2012.
- [24] C. W. Potter, D. Lew, J. McCaa, S. Cheng, S. Eichelberger, and E. Gritmit, "Creating the dataset for the western wind and solar integration study (USA)," *Wind Eng.*, vol. 32, no. 4, pp. 325–338, 2008.
- [25] A. Papavasiliou and S. S. Oren, "Multiarea stochastic unit commitment for high wind penetration in a transmission constrained network," *Oper. Res.*, vol. 61, no. 3, pp. 578–592, May/June 2013.
- [26] J. M. Morales, A. J. Conejo, and J. Perez-Ruiz, "Simulating the impact of wind production on locational marginal prices," *IEEE Trans. Power Syst.*, vol. 26, no. 2, pp. 820–828, May 2011.
- [27] Energinet Wholesale Market Data [Online]. Available: energinet.dk/EN/EI/Engrosmarked/Udtraek-af-markedsdata/Sider/default.aspx
- [28] The Danish Energy Agreement of March 2012 [Online]. Available: www.ens.dk/sites/ens.dk/files/dokumenter/publikationer/downloads/acc-elerating_green_energy_towards_2020.pdf
- [29] E. V. McGarrigle, J. P. Deane, and P. G. Leahy, "How much wind energy will be curtailed on the 2020 Irish power system?," *Renew. Energy*, vol. 55, pp. 544–554, Jul. 2013.
- [30] R. E. Rosenthal, GAMS—A User's Guide, GAMS Development Corp., Washington, DC, USA, Jul. 2013.
- [31] Z. Li and H. Daneshi, "Some observations on market clearing price and locational marginal price," in *Proc. IEEE PES General Meeting*, San Francisco, CA, USA, Jun. 2005.

Hrvoje Pandžić (S'06–M'12) received the M.E.E. and Ph.D. degrees from the Faculty of Electrical Engineering University of Zagreb, Croatia, in 2007 and 2011, respectively.

He is currently an Assistant Professor at the Faculty of Electrical Engineering, University of Zagreb, Croatia. From 2012 to 2014, he was a postdoctoral researcher at the University of Washington, Seattle, WA, USA.

Yishen Wang (S'12) received the B.S. degree from the Department of Electrical Engineering, Tsinghua University, Beijing, China, in 2011. He is currently pursuing the Ph.D. degree in Electrical Engineering at the University of Washington, Seattle, WA, USA.

His research interests include wind integration, wind forecasting, optimization techniques applied to power systems, and power system economics.

Ting Qiu (S'12) received the B.S. degree in control science and engineering from Xi'an University of Technology, China, in 2008 and the M.Sc. degree in system engineering from Xi'an Jiaotong University, China, in 2011. She is currently pursuing the Ph.D. degree in electrical engineering at the University of Washington, Seattle, WA, USA.

Her research interests include optimization algorithms and their applications in electric power system and market operation.

Yury Dvorkin (S'12) received the B.S. degree in electrical engineering from Moscow Power Engineering Institute (National Research University), Moscow, Russia, in 2010. Currently he is pursuing the Ph.D. degree at the University of Washington, Seattle, WA, USA.

He is a Research Assistant at the University of Washington. His research interests revolve around power system economics and flexibility.

Daniel S. Kirschen (M'86–SM'91–F'07) received the electrical and mechanical engineer's degrees from the Université Libre de Bruxelles, Belgium, in 1979, and the M.Sc. and Ph.D. degrees from the University of Wisconsin, Madison, WI USA, in 1980 and 1985, respectively.

He is currently Close Professor of Electrical Engineering at the University of Washington, Seattle, WA, USA. His research focuses on smart grids, the integration of renewable energy sources in the grid, power system economics, and power system security.